forests

MDPI

Article

Physiological and Growth Responses to Increasing Drought of an Endangered Tree Species in Southwest China

Wuji Zheng [1], Xiaohua Gou [1,*], Jiajia Su [1], Haowen Fan [1], Ailing Yu [1], Wenhuo Liu [2], Yang Deng [1], Rubén D. Manzanedo [3,4] and Patrick Fonti [5]

1 Key Laboratory of Western China's Environmental Systems (Ministry of Education), College of Earth and Environmental Sciences, Lanzhou University, Lanzhou 73000, China; zhengwj16@lzu.edu.cn (W.Z.); sujj16@lzu.edu.cn (J.S.); fanhw13@lzu.edu.cn (H.F.); yual16@lzu.edu.cn (A.Y.); dengy@lzu.edu.cn (Y.D.)

2 State Key Laboratory of Cryospheric Sciences, Northwest Institute of Eco-Environment and Resources, Chinese Academy of Sciences, Lanzhou 73000, China; liuwh10@lzu.edu.cn

3 Biology Department, University of Washington, Seattle, WA 98195-1800, USA; rdmanzanedo@fas.harvard.edu

4 Harvard Forest, Harvard University, Petersham, MA 01366, USA

5 Swiss Federal Institute for Forest, Snow and Landscape Research, WSL, 8903 Birmensdorf, Switzerland; patrick.fonti@wsl.ch

* Correspondence: xhgou@lzu.edu.cn; Tel.: +86-0931-891-2404

Received: 2 May 2019; Accepted: 13 June 2019; Published: 17 June 2019

Abstract: *Research Highlights:* We compared annually resolved records of tree-ring width and stable isotope of dead and surviving *Fokienia hodginsii* (Dunn) Henry et Thomas trees. We provide new insights into the relationships and sensitivity of tree growth to past and current climate, and explored the underlying mechanism of drought-induced mortality in *F. hodginsii*. *Background and Objectives:* Drought-induced tree decline and mortality are increasing in many regions around the world. Despite the high number of studies that have explored drought-induced decline, species-specific responses to drought still makes it difficult to apply general responses to specific species. The endangered conifer species, *Fokienia hodginsii*, has experienced multiple drought-induced mortality events in recent years. Our objective was to investigate the historical and current responses to drought of this species. *Materials and Methods:* We used annually resolved ring-width and $\delta^{13}C$ chronologies to investigate tree growth and stand physiological responses to climate change and elevated CO_2 concentration (C_a) in both dead and living trees between 1960 and 2015. Leaf intercellular CO_2 concentration (C_i), C_i/C_a and intrinsic water-use efficiency (iWUE) were derived from $\delta^{13}C$. *Results:* $\delta^{13}C$ were positively correlated with mean vapor pressure deficit and PDSI from previous October to current May, while ring widths were more sensitive to climatic conditions from previous June to September. Moreover, the relationships between iWUE, basal area increment (BAI), and C_i/C_a changed over time. From 1960s to early 1980s, BAI and iWUE maintained a constant relationship with increasing atmospheric CO_2 concentration. After the mid-1980s, we observed a decrease in tree growth, increase in the frequency of missing rings, and an unprecedented increase in sensitivity of ^{13}C and radial growth to drought, likely related to increasingly dry conditions. *Conclusions:* We show that the recent increase in water stress is likely the main trigger for the unprecedented decline in radial growth and spike in mortality of *F. hodginsii*, which may have resulted from diminished carbon fixation and water availability. Given that the drought severity and frequency in the region is expected to increase in the future, our results call for effective mitigation strategies to maintain this endangered tree species.

Keywords: drought; *Fokienia hodginsii*; Southwest China; tree mortality; tree-ring; water-use efficiency; $\delta^{13}C$

1. Introduction

Although forests are the most productive among the terrestrial ecosystems, climate change poses a serious threat to their health. The average global surface temperature has increased by 0.85 °C since the industrial revolution and model-based climate projections for the 21st century anticipate further warming, while changes in precipitation are expected to differ more regionally, increasing in the equatorial Pacific and high latitudes, and decreasing in some subtropical dry and mid-latitude regions [1,2]. Although climate warming may increase the growth of plants in some temperate ecosystems [3], some geographic regions may experience increased drought and heatwaves under certain model projections, threatening the health of those ecosystems [4]. Droughts associated with shifts in precipitation patterns and increasing temperatures could result in a widespread reduction in tree vigor and growth [5] and a reduction in primary productivity [6]. As a result, forest mortality and vegetation shifts are expected to occur in the upcoming decades in many regions across the globe [7–9].

To better forecast these future forest changes, it is crucial to understand the mechanisms by which trees have adapted and survived through a dry climate. However, species-specific responses to drought may complicate the understanding of drought-induced changes in forests [10,11]. Despite a wealth of research in the responses of trees species to drought, there is still no general theory to indicate how a particular species may respond to increasing drought. Therefore, species-specific research is still deeply needed, especially for endangered species that may be particularly threatened by drought.

Fokienia hodginsii serves as a good example of an endangered tree species that may be threatened under increased drought. *F. hodginsii* is the only extant species of its genus. It is an endangered species in southern China and Vietnam with important ecological and commercial value. It is also appreciated for its long lifespan and capacity to grow in marginal environments. At present, its natural distribution range is very narrow and, in most populations, it coexists with evergreen broad-leaved forest species. It is, therefore, critical to understand the influence of changing climate, especially drought, on *F. hodginsii* growth to predict its response to future environmental change, protection, and to provide sound management recommendation for the species in the future. A previous study has shown the drought-related response of *F. hodginsii* to climate change in southern China, but the physiological mechanisms causing tree death are still poorly understood, mainly due to a lack of historical information for the species [12].

Tree-ring data provide an invaluable data source to retrospectively investigate tree growth and physiological responses to climate change. The concentration ratio of stable carbon isotopes ($\delta^{13}C$) in tree rings is influenced by the photosynthetic rate (A) and the stomatal conductance (g_s), both of which are influenced by changes in environmental conditions [13,14]. They are particularly useful for understanding the ecological and physiological changes associated with drought and the mechanisms that cause decline and death [15–17]. Consequently, exploring $\delta^{13}C$ in wood tissues is a way to investigate the long-term impact of the environment on tree growth. Intrinsic water-use efficiency (iWUE), which represents the ratio of A to g_s, reflects the relationship between fixed carbohydrates and water consumed by plants [18,19]. It is a comprehensive physiological and ecological indicator for evaluating the appropriateness of plant growth. Higher iWUE can result from reducing g_s, increasing A, or a combination of the two processes [20]. Previous tree-ring studies have confirmed that the growth of now-dead trees was reduced to some extent already before the death, while iWUE derived from $\delta^{13}C$ values was higher [21–23].

Based on previous research, we hypothesized that dying trees would have higher values of $\delta^{13}C$ and iWUE. We aimed to study the changes in growth behavior and sensitivity of *F. hodginsii* trees to historical drought events based on annually resolved radial growth and $\delta^{13}C$ data. Specifically, we addressed the following questions: (1) What climatic factors affect the radial growth and isotopic signature of *F. hodginsii*; and (2) Can the mechanisms underlying the observed tree decline and mortality be elucidated via combining study of radial growth and iWUE analyses?

2. Data and Methods

2.1. Research Area

We conducted our survey at the Xi Shui National Nature Reserve (105°50′–106°29′ E, 28°07′–28°34′ N, 420–1756 m asl), to the northwest of Guizhou province in Southwest China (Figure 1). The reserve was established in 1994 to conserve natural monsoon evergreen broad-leaved forests of the central subtropics. This area has a typical subtropical monsoon climate (Figure 2), and averages 1094 mm annual precipitation, 68.4% of which falls during the wet season (May–September). Annual mean relative humidity is 84.2%. Annual mean temperature is 13.3 °C, with the lowest mean monthly temperature in January (2.7 °C), and the highest in July (23 °C). It has an undulating topography with steep hills, and shallow soils characterized by low water retention.

F. hodginsii is one of the dominant evergreen conifer tree species in this area. It commonly shares the canopy of dense mixed evergreen and deciduous forests with species such as *Pinus massoniana* Lamb., *Pinus fenzeliana* Hand.-Mazz, and *Cunninghamia lanceolata* (Lamb.) Hook. *F. hodginsii* is distributed primarily in Vietnam and southern China, and it is now recognized in China as an endangered species due to a prolonged and intensive logging history [24]. *F. hodginsii* populations in the study area are perhaps amongst the highest latitude naturally occurring ones of the species (Supporting Information Figure S1).

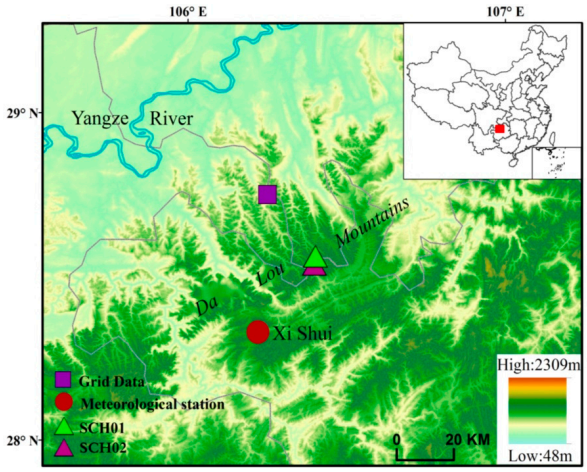

Figure 1. Location of the study sites in the northern part of southwest China. The sampling sites, grid data (28.75° N, 106.25° E), and nearest meteorological station (Xi Shui) are also shown. The overall location of the research region is shown in the inset map.

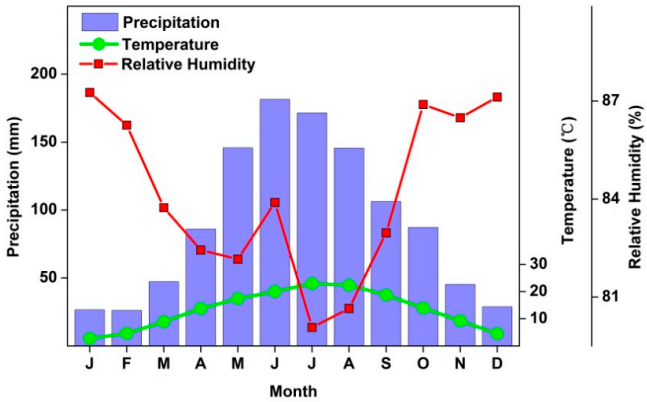

Figure 2. Annual climate conditions for Xi Shui station (see location in Figure 1) from 1960 to 2015 showing total monthly precipitation, mean monthly temperature, and mean monthly relative humidity.

2.2. Climate Data

The closest meteorological station to our study sites (~30 km) is Xi Shui, from which we could obtain monthly climate data from 1960 to 2015, including mean temperature (T), total precipitation (P), relative humidity (RH), and sunshine hours (SH). Temperature and RH data helped compute the vapor pressure deficit (VPD = saturation vapor pressure (e_s) at air temperature, minus the actual (e_a) vapor pressure), one of the main regulators of stomatal activity:

$$VPD = e_s - e_a, \quad (1)$$

Here $e_s = 0.611 \times 10\hat{}(7.5 \times T/(237.3 + T))$ and $e_a = (RH/100) \times e_s$. T is the mean temperature, in degrees Celsius (°C); and RH the relative humidity, in %. Additionally, we obtained data from the CRU (Climate Research Unit, University of East Anglia) TS v. 4.01 on monthly wet days duration (WDD), cloud cover (CC), Standardised Precipitation-Evapotranspiration Index (SPEI), and self-calibrating Palmer Drought Severity Index (scPDSI), available at http://climexp.knmi.nl.

2.3. Core Sampling and Analysis

Our tree-ring data was collected from living and dead trees (Table 1), sampled in November of 2014 and 2016 [12], at 1200–1270 m altitude range within the Xi Shui National Nature Reserve (Figure 1). Dead trees were collected in a precipitous slope in Wangxiantai (SCH01), a scenic area. Trees were still standing and had no green needles remaining in their crown. It is known that most of these mature *F. hodginsii* trees died in recent years (2007 to 2013) [12,25,26]. Not all dead trees were sampled because of the rapid wood decay rate in this subtropical monsoon climate. Only ten out of the total 17 dead trees were cross-dated accurately from pith to bark, the period in which tree death occurred can be generally represented. As *F. hodginsii* trees in SCH01 were almost all dead, and would have been difficult to compare with the living trees. We collected living trees in SCH02, which was environmentally similar to SCH01. SCH02 is located ca. 3 km away from SCHO1, which we hope makes this a useful comparison. SCH02, however, had no standing dead trees. Two or three increment cores per tree were sampled at breast height (1.3 m). Cores were air-dried and sanded before the ring-widths were measured with a precision of 0.001 mm. We used COFECHA software [27] to statistically verify the tree-ring cross-dating. Dead and living trees cross-dated well with each other, giving us the chance to use a single conflated chronology. We used the ARSTAN software to standardize the ring-width series [28], using a negative exponential or linear growth curve to eliminate nonclimatic signals [29]. Subsequently, the biweight robust mean method was employed to merge the detrended index series into a standard (STD) chronology.

For each tree-ring value we also estimated the annual basal area increment (BAI) from pith to bark by assuming concentric tree rings as [30]:

$$BAI = \pi - ({R_n}^2 - {R_{n-1}}^2), \quad (2)$$

where R is the radius of the ring width from trees selected based on distinct growth rings in a given year, and n is the year of tree-ring formation.

Table 1. Characteristics of sampling sites.

Sites	Dead or Living	Latitude (N)	Longitude (E)	Elevation (m a.s.l.)	Cores/ Trees	Slope (°)	Slope Aspect	Time Span (a)
SCH01	Dead	28°33′44″	106°24′05″	1200–1270	30/17	40	Southwest	125.3
SCH02	Living	28°32′14″	106°23′54″	1200–1240	38/18	40	Southwest	89.4

2.4. Carbon Isotope Chronology and Calculations for iWUE

Five trees (three dead trees and two living trees), with no absent rings or obvious growth disturbances that could alter our measurements, were selected for the $\delta^{13}C$ analysis (Table 2). The resulting $\delta^{13}C$ chronologies covered a common period from 1960 to 2007. We extracted wood material for each annual ring using a sharp blade under a binocular microscope. Each ring was further separated into small sections and packed into centrifuge tubes for further chemical treatment. We extracted alpha-cellulose content using the "acetic acid: nitric acid mixture" method based on an extraction method of Jayme-Wise, optimized by Brendel et al. [31]. For the $\delta^{13}C$ analysis, the samples were packed into tin capsules, with a sample weight ranging from 0.09 to 0.12 mg. The $\delta^{13}C$ values were determined at Lanzhou University using a Flash Elemental Analyzer (Flash 2000) coupled with a Thermo Scientific MAT 253 (Thermo Electron Corporation, Bremen, Germany, precision 0.1‰). The Graphite standard ($\delta^{13}C$ = −16‰) was used to calibrate the tree-ting $\delta^{13}C$ values. The ratio of ^{13}C to ^{12}C ($\delta^{13}C$) is expressed in parts per thousand (‰), as:

$$\delta^{13}C = [(R_{sample} / R_{standard}) - 1] \times 1000 \quad (3)$$

where R_{sample} and $R_{standard}$ represent the $^{13}C/^{12}C$ ratios in the sample and in the Vienna Pee Dee Belemnite (VPDB) standard, respectively. The standard deviation of our isotope measurements was 0.05‰.

Table 2. Characteristics of the selected dead and live trees used in carbon isotope measurements.

Cores ID	Dead or Alive	Time Span (years)	Mean Ring Width (mm)	Diameter at Breast Height (cm)	Height (m)	Canopy Position
WXT01B	dead	1877–2007	1.53	45	19.0	dominant
WXT02A	dead	1847–2007	1.42	49	23.0	dominant
WXT27A	dead	1875–2010	1.07	32	20.5	dominant
WXT34C	alive	1889–2016	1.31	37	16.5	codominant
WXT38A	alive	1895–2016	1.50	39	15.0	codominant

The raw $\delta^{13}C$ chronology showed a decreasing trend attributed to the rise of ^{13}C-depleted atmospheric CO_2 due to fossil fuel burning and deforestation since industrialization (the Suess effect). The Suess effect was adjusted by amending individual tree-ring raw $\delta^{13}C$ back to preindustrial settings [32] using the following equation:

$$\delta^{13}C_{corr} = \delta^{13}C_{plant} - (\delta^{13}C_{atm} + 6.4) \quad (4)$$

where C_{corr} is the corrected $\delta^{13}C$ of plant. $\delta^{13}C_{plant}$ and $\delta^{13}C_{atm}$ are the stable carbon isotopic values of plant cellulose and ambient air, respectively.

The intrinsic water use efficiency (iWUE) is the ratio between carbon assimilation rate (A, photosynthesis), and stomatal conductance (g_s). iWUE informs on the long-term trends in the internal regulation of carbon uptake and water loss of plants. iWUE for each ring can be estimated by $\delta^{13}C$ values using the equation:

$$iWUE = A/g_s = C_a \times [b - (\delta^{13}C_{atm} - \delta^{13}C_{plant})]/[(b - a) \times 1.6] = (C_a - C_i)/1.6 \quad (5)$$

where C_a and C_i are the atmospheric and intercellular CO_2 concentrations; a (≈4.4‰) and b (≈27‰) are the diffusion-induced and biochemical fractionations, respectively [13,14].

2.5. Climate-Growth Relationships

Pearson correlation analyses were used to characterize the relationship between $\delta^{13}C$ values and radial growth and climate, with both monthly (from previous March to current October) and seasonal variables (spring: March–May, summer: June–August, fall: September–November, winter:

December–February). We specifically tested the relationship with total precipitation, mean temperature, wet days duration, scPDSI, sunshine hours, relative humidity, potential evaporation, and SPEI6. The temporal stability of the climate-growth and isotope-growth relationships were explored via 21-year running correlation analyses, applied to the chronologies and meteorological data. To explore the potential effects of climate change, we also divided the time series into two approximately equal periods (1960–1984 and 1985–2010) and applied simple linear regression models for each of them and quantified the temporal variation in the $\delta^{13}C$ chronology responses with changing climate. We followed the same methodology, using C_i, C_i/C_a, iWUE, and BAI as response variable to assess their temporal trends.

3. Results

3.1. Climatic Characteristic

The study area has become drier since the late 1980s as RH and PDSI decreased (Figure 3; Supporting Information Table S1). Since 1960, Xi Shui station show similar climatic trends than those of other places in southwestern China [33,34], with increasing temperature (slope = 0.016 °C/year, $R^2 = 0.28$, $p < 0.01$), while the annual precipitation and sunshine hours had no significant trends. Annual VPD also increased significantly (slope = 0.001 hPa/year, $R^2 = 0.13$, $p < 0.01$). Consistent with the VPD increase, though less pronounced (only spring and autumn), annual RH showed a negative trend, with a maximum decrease rate at −0.069%/year ($R^2 = 0.20$, $p < 0.01$) in autumn. Detailed climatic conditions in the study area are shown in the Supporting Information Table S1.

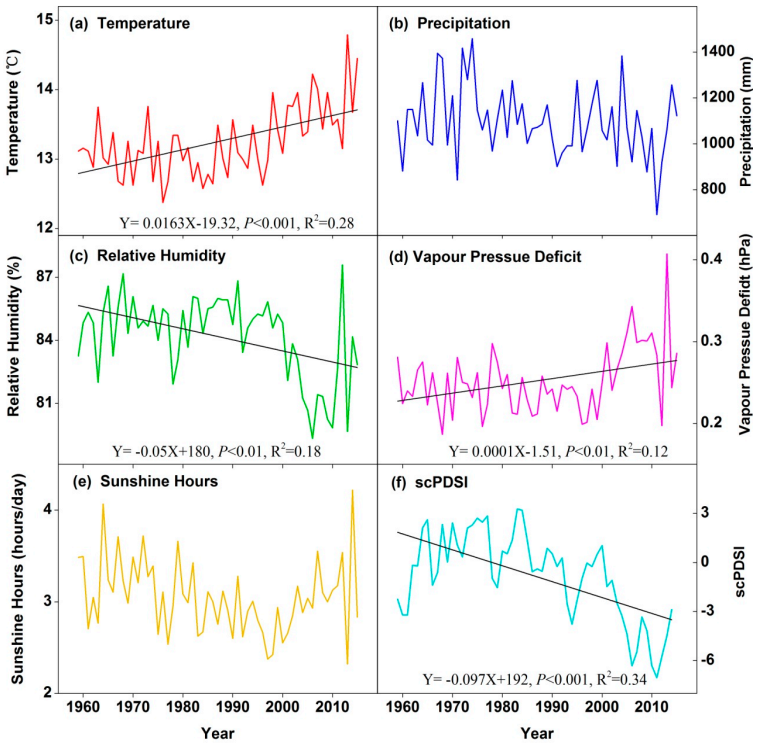

Figure 3. Climatic characteristic in the Xi Shui meteorological station from 1960 to 2015. (**a**) Annual mean temperature; (**b**) annual total precipitation; (**c**) relative humidity; (**d**) vapor pressure deficit; (**e**) annual sunshine hours; (**f**) Annual scPDSI. Linear regression lines and regression parameters are shown for the significant relationships ($p < 0.05$).

3.2. Temporal Characteristics of $\delta^{13}C$ and STD Chronologies

The raw $\delta^{13}C$ series had a decreasing trend (a slope of linear regression: −0.0156 ‰ year^{-1}) from 1960 to 2007, ranging from −24.13‰ to −21.44‰ (Figure 4a) due to the Suess effect. The overall average was −22.55‰ (standard deviation = 0.58). After adjusting for the Suess effect, the $\delta^{13}C_{corr}$ series did not reveal an overall trend. Figure 4b shows the individual and the mean $\delta^{13}C_{corr}$ series after adjusting for the atmospheric $\delta^{13}C$.

The growth chronology showed a drastic reduction in radial growth from 2005 to 2014, consistent for both dead and living trees (Figure 4 and Supporting Information Figure S2), corresponding with a ten-year drought period in the study area (Figure 3). The average annual tree-ring index from 2005 to 2014 is 0.52, substantially lower than the long-term mean and the mature *F. hodginsii* also died in this time period.

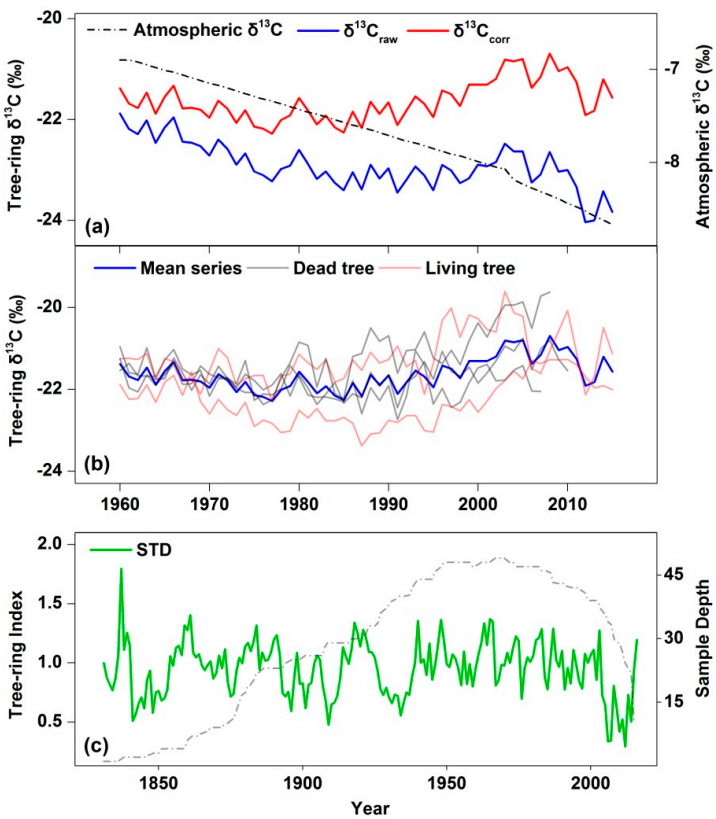

Figure 4. The temporal characteristics of $\delta^{13}C$ chronology and growth chronology (STD). (**a**) $\delta^{13}C_{corr}$ series (red line), the $\delta^{13}C_{raw}$ series (blue line), and the atmospheric $\delta^{13}C$ (dashed line) during 1960–2015; (**b**) individual series of dead trees (black lines) and living trees (red lines), and tree-ring $\delta^{13}C$ chronology (blue line). (**c**) STD chronology (green line) and sample size (dotted line).

3.3. Climate Response of STD and $\delta^{13}C$ Chronologies

Our results indicated a tight connection between the growth of *F. hodginsii* and drought and heat-induced water stress (Figure 5). Tree growth showed a consistently significant negative relationship with VPD and T for the whole period from previous June to September, while higher RH significantly increased growth from previous June to September ($p < 0.001$) (Figure 5a). The effect of SPEI6 was mainly positive and concentrated in the period from previous July to current February, with the strongest correlations ($p < 0.01$) found with conditions during previous autumn and winter (SPEI at other timescales is shown in Supporting Information Figure S3). All monthly scPDSI (previous March–current October) were positively correlated with tree growth, with the strongest being that of previous autumn conditions ($R = 0.63$, $p < 0.001$).

The $\delta^{13}C$ chronology responded more strongly to the climate conditions from previous autumn to current spring (Figure 5b). The $\delta^{13}C$ chronology showed significant and positive responses to VPD from previous October to current May, and significant and negative responses to RH from previous September to current May. Interestingly, aridity, measured as monthly scPDSI, had a very consistent and strong effect during all of the studied periods (previous March–current October), being strongly negatively correlated with $\delta^{13}C$. The highest correlation was found with conditions during the dry season (previous November–current March) ($R = -0.63$, $p < 0.01$). Overall, these results indicate that water conditions from the previous winter to the current spring are the most influential on $\delta^{13}C$ for *F. hodginsii*.

Additionally, growth and $\delta^{13}C$ responses to seasonal conditions were consistent with that of monthly variables, with slightly higher correlation coefficients (Figure 5). Overall, our results highlight the strong effect that water availability during previous growth seasons and early growing seasons exerts on radial growth and $\delta^{13}C$ values.

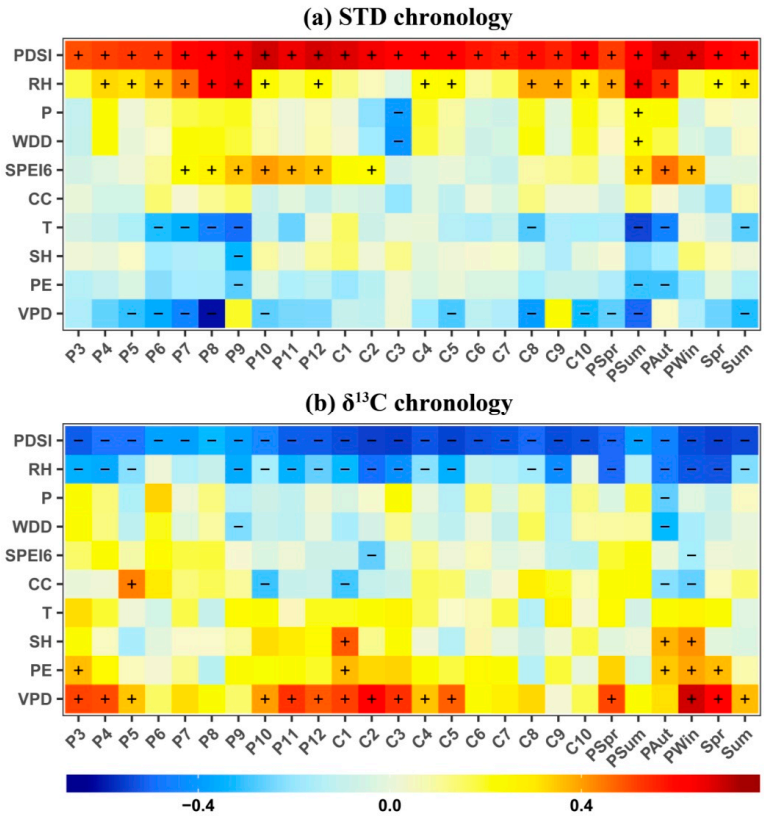

Figure 5. Monthly correlation coefficients of $\delta^{13}C$ and standard (STD) chronologies to climate variables from 1960 to 2015. (**a**) Correlation coefficients between STD chronology and relative humidity (RH), precipitation (P), wet days duration (WDD), drought index at six-month scales (SPEI06), cloud cover (CC), mean temperature (T), sunshine hours (SH), and vapor pressure deficit (VPD) from previous March (P3) to current October (C10) between 1960 and 2015. Correlations with seasonal variables are also shown. Positive and negative correlations at the 95% significantly levels are highlighted with "+" or "–" respectively. (**b**) Correlations between $\delta^{13}C$ chronology and the same climatic factors used in (**a**).

The 21-year running correlation analyses of $\delta^{13}C$ and tree growth with climate variables suggested that growth-climate and isotopic composition-climate relationships were highly unstable and showed an increasing response to drought over the studied period (Figure 6). The correlation values between $\delta^{13}C$, radial growth, and climate (RH, precipitation, VPD as well as SPEI) were mostly not significant before the mid-1980s. Since then, correlation coefficients sharply increased and became highly significant (Figure 6). This change is consistent with the trends of climate (Figure 6), suggesting that

the high correlation after the mid-1980s is likely related to drier climatic conditions associated with increasing temperatures and VPD and decreasing precipitation, RH and, consequently, scPDSI (Table S1 and Figure 3).

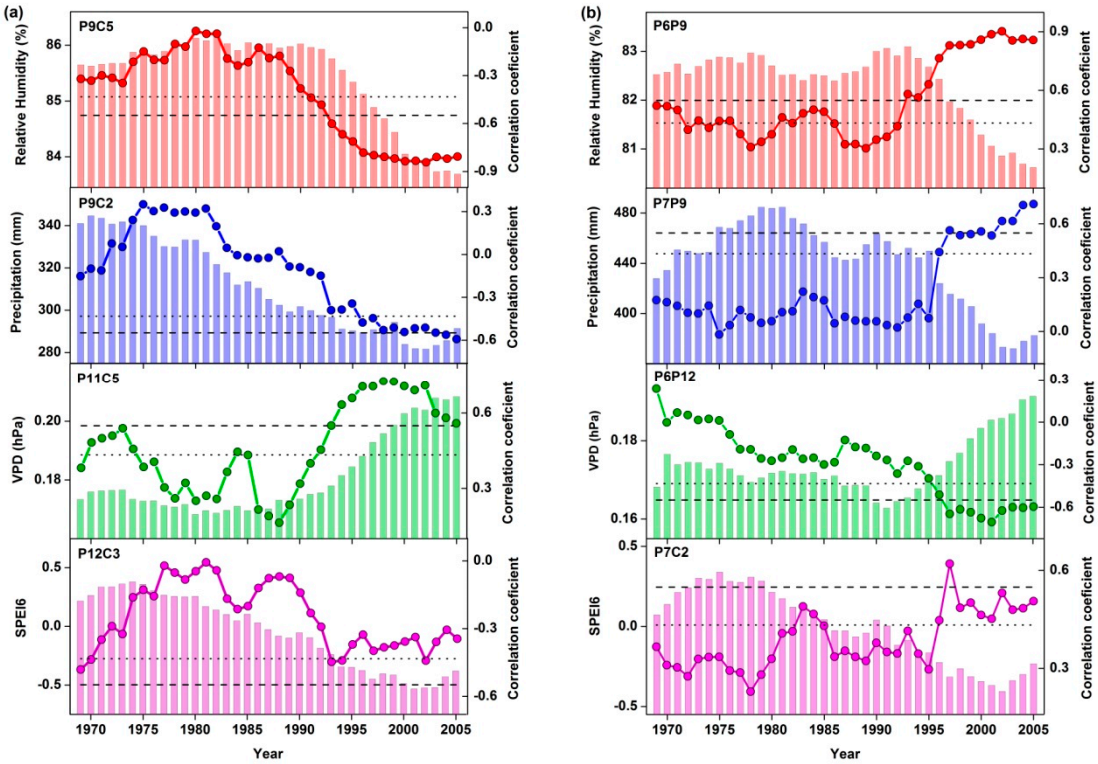

Figure 6. Running correlation analyses for δ^{13}C-climate and tree growth–climate relationships. X-axis indicated the center of the 21-year moving window. Bars show the mean value of the climatic variables for each window. Lines with dotted symbol show the corresponding correlation coefficient. Dotted and dashed horizontal lines indicate significance levels at 95% and 99%, respectively. (**a**) 21-year running correlations between the δ^{13}C chronology and RH (P9C5: previous September–current May), precipitation (P9C2: previous September–current February), VPD (P11C5: previous November–current May), and SPEI6 (P12C3: previous December–current March) during 1960–2015. (**b**) 21-year running correlations between growth (STD chronology) and RH (P6P9: previous June–September), precipitation (P7P9: previous July–September), VPD (P6P12: previous June–December), and SPEI6 (P7C2: previous July–current February) during 1960–2015. The choice of the period was based on the statistical significance of the climate–growth correlations (see Figure 5).

3.4. Temporal Variations in C_a, C_i, C_i/C_a, BAI, STD, and iWUE and Their Correlations with Climate.

During the past 60 years, C_a increased from 310 to 404 μmol mol^{-1}, while iWUE and BAI showed contrasting trends in each period (Figure 7a). During the relatively wet period between 1960 and 1984, C_i increased with increasing atmospheric CO_2, iWUE remained stable (Figure 7c), consistent to the C_i/C_a trend (Figure 7b), and BAI remained consistently high (Figure 7d). However, from 1985 to 2010, radial growth decreased abruptly and reached its lowest value in 2010 at about 45% lower than the long-term average. This happened despite continuously increasing CO_2 concentrations, and was observed both on dead and living trees (Supporting Information Figure S3). During this period, C_i patterns were no longer consistent with increasing atmospheric CO_2, showing no obvious trend, while iWUE increased significantly. Tree mortality events occurred between 2007 and 2013 (Figure 7e), coinciding with unusually dry and warm climate conditions. Similarly, almost all of the missing rings we observed occurred during this period. After 2010, tree growth increased rapidly at the same time as the climate got wetter, and C_i increased, accompanied by rising atmospheric CO_2, while iWUE kept

stable at high levels. This is not caused by the dead trees' lower growth being removed and increasing the average (Supporting Information Figure S3).

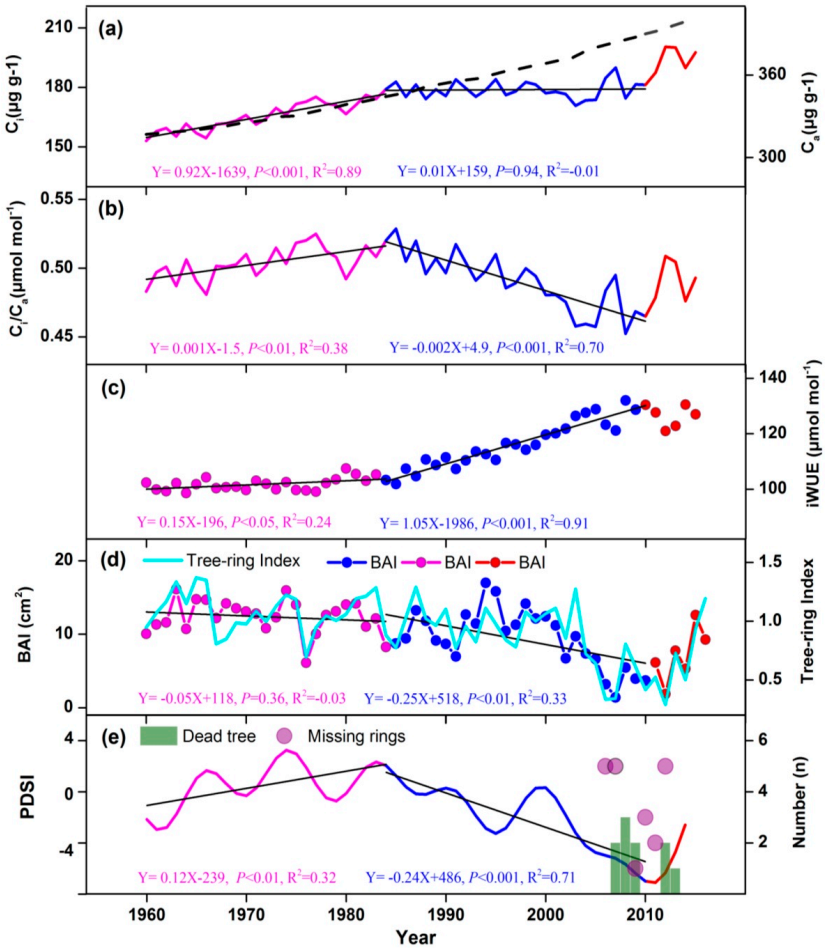

Figure 7. Temporal trends in C_a, C_i, C_i/C_a, BAI, and iWUE. Linear regressions are plotted for the periods 1960–1984 (purple), and 1985–2010 (blue), with their respective *p* and R^2 values. (**a**) The relationship between C_i (solid line) and C_a (dash line). Temporal trend in C_i/C_a (**b**), and iWUE (**c**). (**d**) Temporal trend of BAI (line with dotted symbol) and STD chronology (light blue line). (**e**) Temporal trend of scPDSI processed with a ten-year low-pass filter. The number of dead trees (green bars) and missing rings (purple circles) are also shown.

4. Discussion

Drought-induced tree decline and mortality is increasing in many parts of the world, which could fundamentally alter the composition [35], structure [9], and biogeography [36] of forests. Recently, mature trees of the endangered species *F. hodginsii* from a natural forest in YGP in southwest China are undergoing large mortality events [12,26]. *F. hodginsii* growing in its range boundary is a good example of an endangered tree species that may be more vulnerable to drought. To develop mitigation strategies and maintain forest productivity, it is important to understand how endangered tree species will respond to severe drought [37]. Our results indicated that water availability during the relatively dry season is the most influential factor on *F. hodginsii's* growth, suggesting that increasing drought might trigger growth reduction and mortality events in southwestern China *F. hodginsii*'s forests.

4.1. Climatic Information Recorded by the Tree-Ring $\delta^{13}C$ Series

As we expected, *F. hodginsii* seems to be highly sensitive to climate, particularly to drought, as the calibrated $\delta^{13}C$ series showed a clear response to the water availability from previous autumn to current spring, whereas high water availability during late summer and autumn in the previous year positively influenced tree growth. The significant association between relative humidity, VPD, and $\delta^{13}C$ values during the preceding winter and current spring suggested that stomatal closure due to water stress may be the key driver that controls the $^{13}C/^{12}C$ ratio. $\delta^{13}C$ values in tree rings reflect the rate of stomatal conductance and photosynthesis not only during the growing season, but also in winter, which makes changes in $\delta^{13}C$ highly informative to understand the process of carbohydrate assimilation during tree growth [14,32]. In this sense, it is important to note that, with the exception of January, monthly temperatures in our area are above the generally considered temperature threshold for photosynthesis (5 °C) [38]. Respiration and transpiration rates may be increased by the high temperatures in autumn and winter in the previous years, limiting radial growth in the subsequent year by consuming carbon storage [39]. Meanwhile, a proper moisture budget from previous June to September seems important for an optimal assimilation of the carbohydrates for the next year's growth since soil moisture is usually adequate to sustain foliage water potential and minimize VPD. Moreover, spring conditions also seemed to play an important role in controlling $\delta^{13}C$ values. Trees should have begun to grow as spring mean temperature is about 13.8 °C (Figure 2) in this area [38,40,41]. Warm and dry spring negatively affected tree growth through enhancing evapotranspiration and water stress [42]. The stress caused by previous June to September climatic conditions on tree growth has also been confirmed in other regions of monsoonal Asia, for instance, in southeast Asia [43,44] and the southeastern Tibetan Plateau [45].

4.2. The Physiological Implications of Radial Growth and iWUE

Rising atmospheric CO_2 is expected to positively influence tree growth by increasing carbon availability, which is referred as the "CO_2 fertilization effect" [46]. The clear upward trend of iWUE during the 20th century may indeed be related to the continuous increase in CO_2 concentration since the industrial revolution [47–49]. However, tree growth response to increasing iWUE is likely to be region-, species-, and even climate scenario-specific [48,50]. In our research area, the climate was relatively humid during the 1960s–1980s, and therefore iWUE values were relative stable because of the high photosynthesis and stomatal conductance. This is likely to have allowed trees to take advantage of the higher carbon availability and thus maintain high BAI levels. However, since the early 1980s, climate has become drier in our study areas, as suggested by the inversion of the relationship between iWUE and growth for *F. hodginsii* from 1985 to 2010. During this long-term drought, *F. hodginsii* trees seem to have adopted a conservative water-use strategy to maintain their metabolism by managing stomatal conductance to minimize water loss, resulting in higher iWUE. Drought, in general, not only influences the water relations and hydraulic properties of plants, but also negatively affects photosynthesis [51], which likely led to a reduction in the *F. hodginsii* stored carbon and a failure to maintain their normal physiological metabolic requirements, resulting in a decreasing growth trend. Increasing iWUE and decreasing radial growth can be strong evidence of warming-induced water stress [48,52–54]. However, after 2011, climate conditions seem to have been more favorable for *F. hodginsii*'s growth. Trees showed lower iWUE values and increasing BAI, which likely indicates increasing stomatal conductance and photosynthate storage. This stresses again the importance of environmental variables, especially of those associated with water stress, on *F. hodginsii*'s growth patterns. The unprecedented increase in iWUE and concurrent decrease of BAI in the extremely drought years in early 21st century and the rapid increase in BAI and relatively constant iWUE with diminishing sensitivity to escalating C_a afterwards, suggest that *F. hodginsii* trees are very sensitive to present and future increases in drought stress.

4.3. Possible Mechanisms of Tree Mortality

The catastrophic mortality event without counterbalancing recruitment [12] and the decrease in tree growth since 2004 (at a minimum value since 1865), indicate that the increase in tree mortality recorded in recent years is likely caused by increasing drought. The main physiological mechanisms for trees to cope with severe drought are the capacity to accumulate sufficient carbohydrate [55–57], a lower vulnerability to hydraulic failure [42,55,58,59], or a combination of both [55]. In the case of some evergreen tree species, such as *F. hodginsii*, it is likely that chronic water stress and prolonged stomatal closure may lead to a reduced photosynthetic rate which also results in a further decrease in stored carbon as respiration continues. Carbohydrate reserves can be then further reduced as carbohydrates are still required to drive phloem transport, maintain turgor, and refill embolized xylem during drought [55]. Thus, reduced carbon storage and available water also affect the tree's defensive ability, and mortality occurs soon as one or more of these processes reach a threshold, with feedback mechanisms potentially hastening this process [55].

Additionally, the high frequency of missing rings during this period, and its absence in previous ones, further supports the idea that climate warming and localized drought is affecting these trees. Missing rings, also known as locally absent rings, are an adaptive mechanism that potentially increases survival rates in extreme drought conditions when the trees exhibit reduced respiratory demand, by decreasing the risk of hydraulic failure [60]. However, the repeated occurrence of missing rings over a short period of time is a strong indicator that trees are frequently encountering environmental conditions outside of its survival limit [61]. If the climate continues to dry in the future, as predicted, it may eventually cause large mortality event of mature *F. hodginsii* due to carbon starvation. It is still unclear why drought tends to have a strong effect on old *F. hodginsii* trees. Perhaps old trees are more exposed to environmental conditions because old trees with crowns above the canopy are exposed to higher solar radiation and leaf-to-air vapor pressure deficits than younger ones (Supporting Information Figure S4) [62,63]. It is also possible that larger trees are more susceptible to water stress, carbon starvation, and biotic agents than the younger lot, because the limiting photosynthesis and carbon storage adaptations brought on by drought [62,64] are also generally affected by tree height [65]. Currently, we cannot conclude whether changing climate was solely responsible for tree mortality, or whether other factors and interactions may also be important.

4.4. Implications for Forest Management and Future Research

Theoretically, iWUE is the ratio between net assimilation and stomatal conductance. Here, we showed a reduction in stomatal conductance likely caused by rising in drought stress. Since the mid-1980s, warmer and drier conditions in our study area seemed to have caused an increase in VPD, a decrease in RH and PDSI, reduced stomatal conductance, thus leading to higher $\delta^{13}C$ and iWUE. Previous studies in other areas of China, such as the western Tianshan Mountains and Xinglong Mountains, have reached similar conclusions [66].

Considering that current climatic projections predict a higher likelihood of stronger and longer drought events [4], important changes in forest growth, biomass, and species composition have to be expected. These impacts can have dramatic consequences, especially for drought-sensitive endangered species, such as *F. hodginsii* in the subtropical coniferous forest of China. The few remnant patches of old-growth *F. hodginsii* forests existing in China are likely to suffer if these predictions realize. It has been suggested by some studies that reducing stand density (via thinning) could slow down the process of tree decline and mortality related to drought (e.g., in dry Mediterranean ecosystems) [67,68]. This could be an interesting management option for *F. hodginsii* forest. However, experimental thinning treatments are still necessary before we can discern whether reducing *F. hodginsii* (or associated species) density would reduce water stress, or lower density would result in higher evaporation and reduction in hydraulic diversity, a key factor for forests to withstand drought [69]. Therefore, further work in these ecosystems is needed to be able to inform the best management strategies to reduce the negative effects of climate change on these populations. The best protection and conservation strategies for

these old-growth forests should be scientifically informed if we aim to maintain the high biological and structural diversity of these areas. It is also important to note the value of these old-growth conifer forest as ecological monitoring sites [70] to continue monitoring the potential impacts of increased drought stress, improve the classification of ecological zoning, and develop more adaptive mitigation strategies to sustain Southern China's subtropical forests.

5. Conclusions

By combining annually resolved tree-ring growth and isotope records of dead and surviving *F. hodginsii*, we provided new insights into the relationships and sensitivity of tree growth to historical and current climate, and explored the underlying mechanism of drought-induced mortality of *F. hodginsii*. Our results suggest that carbon assimilation and radial growth are strongly drought-limited. For example, the water accumulated from previous growing seasons affected early growth in subsequent years. The stable relationship between radial growth and iWUE in the 1960s–1980s illustrates that trees can benefit from suitable climate conditions. However, warm and dry conditions between 1985 and 2010 severely affected radial growth, increased iWUE, and decreased tree sensitivity to elevated C_a. The strong response of *F. hodginsii*'s radial growth and associated tree mortality to the early 21st century water limitations does not paint an optimistic future for the species, of which only remnant patches remain within some protected areas. Given that drought in the region is expected to further increase in frequency and intensity in the near future, urgent measures should be taken to ensure the preservation of this valuable tree species.

Supplementary Materials: The following are available online at http://www.mdpi.com/1999-4907/10/6/514/s1, Figure S1: Photos of the sampling sites. (a)–(c) Photos show the habitat of the SCH02 site. (d)–(h) Photos show some dead F. hodginsii trees in the SCH02 site. (i) A living young F. hodginsii trees in SCH02. F. hodginsii, one of the dominant conifer tree species together with Pinus massoniana, Pinus fenzeliana and Cunninghamia lanceolata, stands tall amidst the dense evergreen deciduous forest canopy, Figure S2: (a) Correlation coefficients between STD chronology and monthly SPEI at different time scales for the period between 1960 and 2015. Correlations with seasonal variables is also shown. (b) Correlations with the same environmental variables as (a) and $\delta^{13}C$. Positive and negative correlations with ≥95% significance level are highlighted with '+' or '−'. respectively, Figure S3: Ring width chronologies of dead (a, 26 cores) and living (b, 24 cores) *Fokienia hodginsii* trees. Blue lines show the detrended ring-width chronologies. Red lines show the mean raw ring width (mm), Table S1: Trends in annual and seasonal temperature, precipitation, relative humidity, vapor pressure deficit, sunshine hours, and Palmer drought severity index (PDSI). Bold type indicates significant linear trends ($p \leq 0.05$), Figure S4: Twenty-one-year running correlations of the SCH01 (yellow line with dotted symbol) and SCH02 (dark line with triangle symbol) with RH (previous September–current May), precipitation (previous September–current February), VPD (previous November–current May), and PDSI (previous November–current May) during 1960–2015. For comparison, a 21-year running mean of the climate variables (Bars) is shown. The s-axis indicates the center of the 21-year window.

Author Contributions: Conceptualization, W.Z., X.G.; investigation, W.Z, J.S., W.L., H.F., and Y.D.; data curation, W.Z.; writing—original draft preparation, W.Z.; writing—review and editing, J.S., R.D.M., A.Y. and P.F.; supervision, X.G.; funding acquisition, X.G.

Funding: This work was supported by the National Natural Science Foundation of China (No. 41475067), the Strategic Priority Research Program of Chinese Academy of Sciences (No. XDA20100102), and the Fundamental Research Funds for the Central Universities (No.lzujbky-2017-it86, No.lzujbky-2017-it94 and No.lzujbky-2017-41). R.D.M. is supported by the Swiss National Science Foundation, through a Post Doc Mobility Grant.

Acknowledgments: We are grateful for the helpful and constructive comments of two anonymous reviewers, the kindly help and reminder from the editor, Annie Zhang. We thank Liang Wei for helping us revise the manuscript. We also thank Fu Gu, Wei Lin who have helped to collect samples.

Conflicts of Interest: The authors declare no conflict of interest.

References

1. IPCC. *Summary for Policymakers of Climate Change 2013: The Physical Science Basis*; Contribution of working group i to the fifth assessment report of the intergovernmental panel on climate change; Cambridge University Press: Cambridge, UK, 2013.

2. Stott, P.A.; Mitchell, J.F.B.; Allen, M.R.; Delworth, T.L.; Gregory, J.M.; Meehl, G.A.; Santer, B.D. Observational constraints on past attributable warming and predictions of future global warming. *Am. Meteorol. Soc.* **2006**, *19*, 3055–3069. [CrossRef]
3. Cox, P.M.; Betts, R.A.; Jones, C.D.; Spall, S.A.; Totterdell, I.J. Acceleration of global warming due to carbon-cycle feedbacks in a coupled climate model. *Nature* **2000**, *6809*, 184. [CrossRef] [PubMed]
4. Bonan, G.B. Forests and climate change: Forcings, feedbacks, and the climate benefits of forests. *Science* **2008**, *320*, 1444–1449. [CrossRef] [PubMed]
5. Martinez-Vilalta, J.; Prat, E.; Oliveras, I.; Pinol, J. Xylem hydraulic properties of roots and stems of nine mediterranean woody species. *Oecologia* **2002**, *133*, 19–29. [CrossRef] [PubMed]
6. Ciais, P.; Reichstein, M.; Viovy, N.; Granier, A.; Ogee, J.; Allard, V.; Aubinet, M.; Buchmann, N.; Bernhofer, C.; Carrara, A.; et al. Europe-wide reduction in primary productivity caused by the heat and drought in 2003. *Nature* **2005**, *437*, 529–533. [CrossRef] [PubMed]
7. Allen, C.D.; Breshears, D.D.; McDowell, N.G. On underestimation of global vulnerability to tree mortality and forest die-off from hotter drought in the anthropocene. *Ecosphere* **2015**, *6*, 1–55. [CrossRef]
8. Choat, B.; Jansen, S.; Brodribb, T.J.; Cochard, H.; Delzon, S.; Bhaskar, R.; Bucci, S.J.; Feild, T.S.; Gleason, S.M.; Hacke, U.G.; et al. Global convergence in the vulnerability of forests to drought. *Nature* **2012**, *491*, 752–755. [CrossRef]
9. Allen, C.D.; Macalady, A.K.; Chenchouni, H.; Bachelet, D.; McDowell, N.; Vennetier, M.; Kitzberger, T.; Rigling, A.; Breshears, D.D.; Hogg, E.H.; et al. A global overview of drought and heat-induced tree mortality reveals emerging climate change risks for forests. *For. Ecol. Manag.* **2010**, *259*, 660–684. [CrossRef]
10. Wei, L.; Xu, C.; Jansen, S.; Zhou, H.; Christoffersen, B.O.; Pockman, W.T.; Middleton, R.S.; Marshall, J.D.; McDowell, N.G. A heuristic classification of woody plants based on contrasting shade and drought strategies. *Tree Physiol.* **2019**. [CrossRef]
11. Adams, H.D.; Zeppel, M.J.B.; Anderegg, W.R.L.; Hartmann, H.; Landhausser, S.M.; Tissue, D.T.; Huxman, T.E.; Hudson, P.J.; Franz, T.E.; Allen, C.D.; et al. A multi-species synthesis of physiological mechanisms in drought-induced tree mortality. *Nat. Ecol. Evol.* **2017**, *1*, 1285–1291. [CrossRef]
12. Su, J.; Gou, X.; Deng, Y.; Zhang, R.; Liu, W.; Zhang, F.; Lu, M.; Chen, Y.; Zheng, W. Tree growth response of fokienia hodginsii to recent climate warming and drought in southwest china. *Int. J. Biometeorol.* **2017**, *61*, 2085–2096. [CrossRef] [PubMed]
13. Farquhar, G.D.; Ehleringer, J.R.; Hubick, K.T. Carbon isotope discrimination and photosynthesis. Annual review of plant biology. *Annu. Rev. Plant Biol.* **1989**, *40*, 503–537. [CrossRef]
14. Farquhar, G.D.; Sharkey, T.D. Stomatal conductance and photosynthesis. *Annu. Rev. Plant Physiol.* **1982**, *33*, 317–345. [CrossRef]
15. Leavitt, S.W.; Long, A. Drought indicated in carbon-13lcarbon-12 ratios of southwestern tree rings. *J. Am. Water Res. Assoc.* **1989**, *25*, 341–347. [CrossRef]
16. Saurer, M.; Siegwolf, R.T.W.; Schweingruber, F.H. Carbon isotope discrimination indicates improving water-use efficiency of trees in northern eurasia over the last 100 years. *Glob. Chang. Biol.* **2004**, *10*, 2109–2120. [CrossRef]
17. Herrero, A.; Castro, J.; Zamora, R.; Delgado-Huertas, A.; Querejeta, J.I. Growth and stable isotope signals associated with drought-related mortality in saplings of two coexisting pine species. *Oecologia* **2013**, *173*, 1613–1624. [CrossRef]
18. Seibt, U.; Rajabi, A.; Griffiths, H.; Berry, J.A. Carbon isotopes and water use efficiency: Sense and sensitivity. *Oecologia* **2008**, *155*, 441–454. [CrossRef]
19. Lévesque, M.; Rigling, A.; Bugmann, H.; Weber, P.; Brang, P. Growth response of five co-occurring conifers to drought across a wide climatic gradient in central europe. *Agric. For. Meteorol.* **2014**, *197*, 1–12. [CrossRef]
20. McCarroll, D.; Gagen, M.H.; Loader, N.J.; Robertson, I.; Anchukaitis, K.J.; Los, S.; Young, G.H.F.; Jalkanen, R.; Kirchhefer, A.; Waterhouse, J.S. Correction of tree ring stable carbon isotope chronologies for changes in the carbon dioxide content of the atmosphere. *Geochim. Cosmochim. Acta* **2009**, *73*, 1539–1547. [CrossRef]
21. Levanic, T.; Cater, M.; McDowell, N.G. Associations between growth, wood anatomy, carbon isotope discrimination and mortality in a quercus robur forest. *Tree Physiol.* **2011**, *31*, 298–308. [CrossRef]
22. Timofeeva, G.; Treydte, K.; Bugmann, H.; Rigling, A.; Schaub, M.; Siegwolf, R.; Saurer, M. Long-term effects of drought on tree-ring growth and carbon isotope variability in scots pine in a dry environment. *Tree Physiol.* **2017**, *37*, 1028–1041. [CrossRef] [PubMed]

23. Navarro-Cerrillo, R.M.; Sarmoum, M.; Gazol, A.; Abdoun, F.; Camarero, J.J. The decline of algerian cedrus atlantica forests is driven by a climate shift towards drier conditions. *Dendrochronologia* **2019**, *55*, 60–70. [CrossRef]
24. Wang, A.; Liu, Y.; Liu, S.; Yang, T. A preliminary report on the geographic distribution of nature forest fokienia hodginsii in china. *Chin. J. Ecol.* **1984**, *4*, 19–23. (In Chinese)
25. Li, M.; Deng, L.; Pan, D.; Mu, J.; Li, C.; Yang, C. Study on growth process of fokienia hodginsii community in xishui nature reserve in guizhou. *J. Anhui Agric.* **2015**, *43*, 199–202. (In Chinese)
26. Li, M.; Deng, L.; Jiang, Y.; Yang, C.; Mu, J. Community composition and structure of fokienia hodginsii community in xishui nature reserve in guizhou. *J. Northwest For. Univ.* **2013**, *28*, 46–50. (In Chinese)
27. Holmes, R.L. Computer-assisted quality control in tree-ring dating and measurement. *Tree-Ring Bull.* **1983**, *43*, 51–67.
28. Cook, E.R. *A Time Series Approach to Tree-Ring Standardization*; University of Arizona: Tucson, AZ, USA, 1985.
29. Fritts, H.C. *Tree Rings and Climate*; Academic Press: Cambridge, MA, USA, 1976.
30. Phipps, R.; Whiton, J. Decline in long-term growth trends of white oak. *Can. J. For. Res.* **1988**, *18*, 24–32. [CrossRef]
31. Brendel, O.; Iannetta, P.P.M.; Stewart, D. A rapid and simple method to isolate pure alpha-cellulose. *Phytochem. Anal.* **2000**, *11*, 7–10. [CrossRef]
32. McCarroll, D.; Loader, N.J. Stable isotopes in tree rings. *Quat. Sci. Rev.* **2004**, *23*, 771–801. [CrossRef]
33. Wang, L.; Chen, W.; Zhou, W.; Huang, G. Teleconnected influence of tropical northwest pacific sea surface temperature on interannual variability of autumn precipitation in southwest china. *Clim. Dyn.* **2015**, *45*, 2527–2539. [CrossRef]
34. Zhang, M.; He, J.; Wang, B.; Wang, S.; Li, S.; Liu, W.; Ma, X. Extreme drought changes in southwest china from 1960 to 2009. *J. Geogr. Sci.* **2013**, *23*, 3–16. [CrossRef]
35. Engelbrecht, B.M.; Comita, L.S.; Condit, R.; Kursar, T.A.; Tyree, M.T.; Turner, B.L.; Hubbell, S.P. Drought sensitivity shapes species distribution patterns in tropical forests. *Nature* **2007**, *447*, 80–82. [CrossRef] [PubMed]
36. D'Orangeville, L.; Duchesne, L.; Houle, D.; Kneeshaw, D.; Cote, B.; Pederson, N. Northeastern north america as a potential refugium for boreal forests in a warming climate. *Science* **2016**, *352*, 1452–1455. [CrossRef] [PubMed]
37. Phillips, O.L.; Aragao, L.E.; Lewis, S.L.; Fisher, J.B.; Lloyd, J.; Lopez-Gonzalez, G.; Malhi, Y.; Monteagudo, A.; Peacock, J.; Quesada, C.A.; et al. Drought sensitivity of the amazon rainforest. *Science* **2009**, *323*, 1344–1347. [CrossRef] [PubMed]
38. Eugene, A.V.; Hughes, M.K.; Alexander, V.S. *Growth Dynamics of Conifer Tree Rings: Images of Past and Future Environments*; Springer Science & Business Media: Berlin, Germany, 2006; p. 351.
39. Rolland, C. Tree-ring and climate relationships for abies alba in the internal alps. *Tree-Ring Bull.* **1993**, *53*, 1–11.
40. Shi, J.; Lu, H.; Li, J.; Shi, S.; Wu, S.; Hou, X.; Li, L. Tree-ring based february–april precipitation reconstruction for the lower reaches of the yangtze river, southeastern china. *Glob. Planet. Chang.* **2015**, *131*, 82–88. [CrossRef]
41. Evans, M.N.; Reichert, B.K.; Kaplan, A.; Anchukaitis, K.J.; Vaganov, E.A.; Hughes, M.K.; Cane, M.A. A forward modeling approach to paleoclimatic interpretation of tree-ring data. *J. Geophys. Res. Biogeosci.* **2006**, *111*, G03008. [CrossRef]
42. Bréda, N.; Huc, R.; Granier, A.; Dreyer, E. Temperate forest trees and stands under severe drought: A review of ecophysiological responses, adaptation processes and long-term consequences. *Ann. For. Sci.* **2006**, *63*, 625–644. [CrossRef]
43. Buckley, B.M.; Anchukaitis, K.J.; Penny, D.; Fletcher, R.; Cook, E.R.; Sano, M.; Nam le, C.; Wichienkeeo, A.; Minh, T.T.; Hong, T.M. Climate as a contributing factor in the demise of angkor, cambodia. *Proc. Natl. Acad. Sci. USA* **2010**, *107*, 6748–6752. [CrossRef]
44. Sano, M.; Buckley, B.M.; Sweda, T. Tree-ring based hydroclimate reconstruction over northern vietnam from fokienia hodginsii: Eighteenth century mega-drought and tropical pacific influence. *Clim. Dyn.* **2008**, *33*, 331–340. [CrossRef]
45. Fan, Z.X.; Bräuning, A.; Cao, K.F. Tree-ring based drought reconstruction in the central hengduan mountains region (China) since a.D. 1655. *Int. J. Climatol.* **2008**, *28*, 1879–1887. [CrossRef]

46. Soule, P.T.; Knapp, P.A. Radial growth rate increases in naturally occurring ponderosa pine trees: A late-20th century CO_2 fertilization effect? *N. Phytol.* **2006**, *171*, 379–390. [CrossRef]
47. Silva, L.C.R.; Anand, M.; Shipley, B. Probing for the influence of atmospheric co_2 and climate change on forest ecosystems across biomes. *Glob. Ecol. Biogeogr.* **2013**, *22*, 83–92. [CrossRef]
48. Andreu-Hayles, L.; Planells, O.; GutiÉRrez, E.; Muntan, E.; Helle, G.; Anchukaitis, K.J.; Schleser, G.H. Long tree-ring chronologies reveal 20th century increases in water-use efficiency but no enhancement of tree growth at five iberian pine forests. *Glob. Chang. Biol.* **2011**, *17*, 2095–2112. [CrossRef]
49. Linares, J.C.; Delgado-Huertas, A.; Julio Camarero, J.; Merino, J.; Carreira, J.A. Competition and drought limit the response of water-use efficiency to rising atmospheric carbon dioxide in the mediterranean fir abies pinsapo. *Oecologia* **2009**, *161*, 611–624. [CrossRef]
50. Manzanedo, R.D.; Ballesteros-Canovas, J.; Schenk, F.; Stoffel, M.; Fischer, M.; Allan, E. Increase in CO_2 concentration could alter the response of hedera helix to climate change. *Ecol. Evol.* **2018**, *8*, 8598–8606. [CrossRef] [PubMed]
51. Chaves, M.M.; Pereira, J.S.; Maroco, J.; Rodrigues, M.L.; Ricardo, C.P.P.; Osório, M.L.; Carvalho, I.; Faeia, T.; Pinheiro, C. How plants cope with water stress in the field? Photosynthesis and growth. *Ann. Bot.* **2002**, *89*, 907–916. [CrossRef]
52. Silva, L.C.; Horwath, W.R. Explaining global increases in water use efficiency: Why have we overestimated responses to rising atmospheric CO_2 in natural forest ecosystems? *PLoS ONE* **2013**, *8*, e53089. [CrossRef]
53. Nock, C.A.; Baker, P.J.; Wanek, W.; Leis, A.; Grabner, M.; Bunyavejchewin, S.; Hietz, P. Long-term increases in intrinsic water-use efficiency do not lead to increased stem growth in a tropical monsoon forest in western thailand. *Glob. Chang. Biol.* **2011**, *17*, 1049–1063. [CrossRef]
54. Peñuelas, J.; Hunt, J.M.; Ogaya, R.; Jump, A.S. Twentieth century changes of tree-ring δ^{13}c at the southern range-edge of fagus sylvatica: Increasing water-use efficiency does not avoid the growth decline induced by warming at low altitudes. *Glob. Chang. Biol.* **2008**, *14*, 1076–1088. [CrossRef]
55. McDowell, N.G.; Beerling, D.J.; Breshears, D.D.; Fisher, R.A.; Raffa, K.F.; Stitt, M. The interdependence of mechanisms underlying climate-driven vegetation mortality. *Trends Ecol. Evol.* **2011**, *26*, 523–532. [CrossRef] [PubMed]
56. Sala, A. Lack of direct evidence for the carbon-starvation hypothesis to explain drought-induced mortality in trees. *Proc. Natl. Acad. Sci. USA* **2009**, *106*, E68. [CrossRef] [PubMed]
57. Breshears, D.D.; Cobb, N.S.; Rich, P.M.; Price, K.P.; Allen, C.D.; Balice, R.G.; Romme, W.H.; Kastens, J.H.; Floyd, M.L.; Belnap, J.; et al. Regional vegetation die-off in response to global-change-type drought. *Proc. Natl. Acad. Sci. USA* **2005**, *102*, 15144–15148. [CrossRef] [PubMed]
58. Meinzer, F.C.; McCulloh, K.A.; Lachenbruch, B.; Woodruff, D.R.; Johnson, D.M. The blind men and the elephant: The impact of context and scale in evaluating conflicts between plant hydraulic safety and efficiency. *Oecologia* **2010**, *164*, 287–296. [CrossRef] [PubMed]
59. Meinzer, F.C.; Johnson, D.M.; Lachenbruch, B.; McCulloh, K.A.; Woodruff, D.R. Xylem hydraulic safety margins in woody plants: Coordination of stomatal control of xylem tension with hydraulic capacitance. *Funct. Ecol.* **2009**, *23*, 922–930. [CrossRef]
60. Liang, E.; Leuschner, C.; Dulamsuren, C.; Wagner, B.; Hauck, M. Global warming-related tree growth decline and mortality on the north-eastern tibetan plateau. *Clim. Chang.* **2015**, *134*, 163–176. [CrossRef]
61. Zhao, S.; Jiang, Y.; Dong, M.; Xu, H.; Manzanedo, R.D.; Pederson, N. Early monsoon failure and mid-summer dryness induces growth cessation of lower range margin picea crassifolia. *Trees* **2018**, *32*, 1401–1413. [CrossRef]
62. McDowell, N.; Pockman, W.T.; Allen, C.D.; Breshears, D.D.; Cobb, N.; Kolb, T.; Plaut, J.; Sperry, J.; West, A.; Williams, D.G.; et al. Mechanisms of plant survival and mortality during drought: Why do some plants survive while others succumb to drought? *N. Phytol.* **2008**, *178*, 719–739. [CrossRef]
63. Fensham, R.J.; Fairfax, R.J. Drought-related tree death of savanna eucalypts: Species susceptibility, soil conditions and root architecture. *J. Veg. Sci.* **2007**, *18*, 71–80. [CrossRef]
64. Phillips, O.L.; van der Heijden, G.; Lewis, S.L.; Lopez-Gonzalez, G.; Aragao, L.E.; Lloyd, J.; Malhi, Y.; Monteagudo, A.; Almeida, S.; Davila, E.A.; et al. Drought-mortality relationships for tropical forests. *N. Phytol.* **2010**, *187*, 631–646. [CrossRef]
65. Niklas, K.J.; Spatz, H.C. Growth and hydraulic (not mechanical) constraints govern the scaling of tree height and mass. *Proc. Natl. Acad. Sci. USA* **2004**, *101*, 15661–15663. [CrossRef]

66. Wu, G.; Liu, X.; Chen, T.; Xu, G.; Wang, W.; Zeng, X.; Wang, B.; Zhang, X. Long-term variation of tree growth and intrinsic water-use efficiency in schrenk spruce with increasing CO_2 concentration and climate warming in the western tianshan mountains, China. *Acta Physiol. Plant.* **2015**, *37*, 150. [CrossRef]
67. Candel-Pérez, D.; Lo, Y.-H.; Blanco, J.; Chiu, C.-M.; Camarero, J.; González de Andrés, E.; Imbert, J.; Castillo, F. Drought-induced changes in wood density are not prevented by thinning in scots pine stands. *Forests* **2018**, *9*, 4. [CrossRef]
68. Grossiord, C. Having the right neighbors: How tree species diversity modulates drought impacts on forests. *N. Phytol.* **2018**. [CrossRef] [PubMed]
69. Anderegg, W.R.L.; Konings, A.G.; Trugman, A.T.; Yu, K.; Bowling, D.R.; Gabbitas, R.; Karp, D.S.; Pacala, S.; Sperry, J.S.; Sulman, B.N.; et al. Hydraulic diversity of forests regulates ecosystem resilience during drought. *Nature* **2018**, *561*, 538–541. [CrossRef] [PubMed]
70. Zhou, G.; Peng, C.; Li, Y.; Liu, S.; Zhang, Q.; Tang, X.; Liu, J.; Yan, J.; Zhang, D.; Chu, G. A climate change-induced threat to the ecological resilience of a subtropical monsoon evergreen broad-leaved forest in southern china. *Glob. Chang. Biol.* **2013**, *19*, 1197–1210. [CrossRef] [PubMed]

© 2019 by the authors. Licensee MDPI, Basel, Switzerland. This article is an open access article distributed under the terms and conditions of the Creative Commons Attribution (CC BY) license (http://creativecommons.org/licenses/by/4.0/).